Research Paper

PEGylated Interferon-α2b: A Branched 40K Polyethylene Glycol Derivative

Jose Ramon,[1] Vivian Saez,[1] Reynier Baez,[1] Raymersy Aldana,[1] and Eugenio Hardy[2,3]

Purpose. The conjugation of interferon-α2b (IFN-α2b) to a branched-chain (40,000) polyethylene glycol (PEG$_{2,40K}$) was studied.

Methods. We studied the conjugation of IFN-α2b at different pH values (6.5, 7, and 8), using the PEG$_{2,40K}$ reagent in either solution or solid state. MonoPEGylated interferon was isolated by ion-exchange chromatography and characterized using (1) sodium dodecyl sulfate-polyacrylamide gel electrophoresis, (2) cation exchange high-performance liquid chromatography, (3) bicinchoninic acid protein assay, (4) enzyme-linked immunosorbent assay, (5) cell-based bioassays, (6) thermal stability (at 60°C), (7) tryptic digestion, and (8) pharmacokinetics in rats.

Results. PEGylation reaction gave 30–55% PEG$_{2,40K}$-IFN-α2b, 1–10% polyPEGylated interferon, and 35–70% unmodified IFN-α2b. Compared to the polyPEGylated IFN-α2b species, the pure (96%) monoPEGylated conjugate retained a significantly higher bioactivity (IU/mg): $1.7 \times 10^4 \pm 8.5 \times 10^3$ *vs.* $2.8 \times 10^6 \pm 1.4 \times 10^6$ for antiviral and $1.9 \times 10^4 \pm 9.5 \times 10^3$ *vs.* $3.1 \times 10^6 \pm 1.6 \times 10^6$ for antiproliferative activity. Immunorecognition against IFN was reduced by the PEG$_{2,40K}$ moiety in the conjugate. This monoPEGylated IFN-α2b, which migrated as a single band in gel electrophoresis, was found to be a heterogeneous, complex mixture of different positional isomers. PEGylation markedly enhanced both the resistance to tryptic degradation and the thermal stability of IFN-α2b. The serum half-life of 40K PEG–IFN was 330-fold longer, while plasma residence time was increased 708 times compared to native IFN.

Conclusion. The PEG$_{2,40K}$ conjugate of IFN-α2b has increased *in vitro* and *in vivo* stability as compared to the native cytokine.

KEY WORDS: branched chain PEG; IFN-α2b; *in vitro* stability; PEGylation; pharmacokinetics.

INTRODUCTION

Interferon (IFN) comprises a family of cytokines with characteristic biological properties, including antiviral, immunoregulatory, and antiproliferative activities (1). IFN-α produced by recombinant DNA technology has undergone extensive clinical investigation which demonstrates the use of this cytokine for treating both viral and oncological human diseases (e.g., hepatitis B and C, hairy-cell leukemia, malignant melanoma, non-Hodgkin's lymphoma, and chronic myelogenous leukemia) (2,3).

The clinical utility of interferon α-based drugs, however, has been limited by the relatively restricted bioavailability of IFN-α proteins (4,5). Indeed, the half-life of IFN-α in human serum is less than 12 hours, with peak serum concentration occurring at 3–8 h following subcutaneous or intravenous administration (6). Given that little or no IFN is detected 24 h after administration, patients often require repeated (e.g., from three times a week to daily) doses to achieve the desired therapeutic benefit for most hepatological or oncological indications (3,4,7,8). Consequently, long-term treatment regimens with IFNs place a burden on the patient and impact his or her quality of life (4,7). Other problems that may also restrict the successful use of IFN-α in therapy are susceptibility to degradation by proteases, immunogenicity, and antigenicity (9).

During the last few years, PEGylation technology has been used to develop long-acting forms of IFN-α that help avoid most of these problems. In the early 1990s, Nalin *et al.* conjugated IFN-α2a to a linear polyethylene glycol (PEG) (M_r 5000) via a urea linkage (10). The half-life and plasma residence time parameters of this conjugate, with reduced immunogenicity in mice (11), were in rats 1.5- and 2-fold greater than those corresponding to the native IFN-α2a (5). In humans, a twice-weekly dosing of PEG$_{5K}$-IFN-α2a is required to achieve antiviral levels similar to those attained with unconjugated IFN, as shown in a phase II trial involving chronic hepatitis C patients (12).

[1] Formulation Development Department, Center for Genetic Engineering and Biotechnology, Havana, Cuba

[2] Vaccine Department, Center for Genetic Engineering and Biotechnology, Havana, Cuba

[3] To whom correspondence should be addressed (e-mail: ehardy@cigb.edu.cu)

ABBREVIATIONS: BCA, bicinchoninic acid; CBB, Coomassie brilliant blue; ELISA, enzyme-linked immunosorbent assay; IEC, ion-exchange chromatography; IFN, interferon; mAb, monoclonal antibody; M_r, average molecular mass; PEG, polyethylene glycol; RP-HPLC, reversed-phase high performance liquid chromatography; SDS-PAGE, sodium dodecylsulfate-polyacrylamide gel electrophoresis.

Gilbert and Park-Cho (1997) used a linear monomethoxy PEG polymer (with an average molecular mass (M_r) of 12,000) to develop an improved PEGylated form of IFN-α2b (13). The PEG_{12K}-IFN-α2b conjugate enhances pharmacokinetic properties in both animals and humans (7). According to a phase I clinical trial with 58 patients, both the serum half-life (40 h) and mean apparent clearance (22 ml/h per kg) of PEG_{12K}-IFN-α2b in serum are considerably improved over native interferon. Following administration, clinically significant levels of the conjugate persisted an entire week, reaching sustained maximal serum concentrations during the first 48–72 h (14). A recent phase III monotherapy trial with 1219 chronic hepatitis C adult patients showed that PEG_{12K}-IFN-α2b given weekly at three different doses (0.5, 1, or 1.5 μg per kg body weight) is superior to the standard, non-PEGylated IFN-α2b in eliminating detectable hepatitis C viral RNA (15).

Similar success has been achieved with the development of another PEGylated form of IFN-α2a. Bailon *et al.* conjugated IFN-α2a with an *N*-hydroxysuccinimide ester derivative of PEG of M_r 40,000 ($PEG_{2,40K}$) (11). The link between the IFN-α2a protein and second-generation $PEG_{2,40K}$ polymer is an amide bond that is stable under physiological conditions, and confers considerable advantage over other reagents such as succinimidyl carbonate or succinate PEG commonly used for protein PEGylation (16). In comparison with native IFN-α2a, the PEGylated ($PEG_{2,40K}$) IFN-α2a form shows improved pharmacokinetic properties, in studies in animals (11) and healthy humans (5). $PEG_{2,40K}$-IFN-α2a has also been shown to exhibit superior clinical efficacy in treating hepatitis C virus-infected patients (5).

Activated $PEG_{2,40K}$ polymer has been used to obtain conjugates of other proteins (e.g., ribonuclease, catalase, trypsin, asparaginase, uricase, Fab' anti-interleukin-8) (17,18) but not of IFN-α2b. Even when the primary structures of interferon-α subvariants 2a and 2b differ by only the amino acid at position 23 (arginine for IFN-α2b and lysine for IFN-α2a (19)) and both subtypes are able to bind the same type I receptor, these IFNs are known to be markedly different. They may differ in their ability to 1) inhibit human cell growth (20), 2) interfere with viral activities (20), and 3) develop antibodies in patients (21); as well as 4) in their receptor-binding site (22).

In this study we explored the conjugation of IFN-α2b to $PEG_{2,40K}$. The resulting $PEG_{2,40K}$-IFN-α2b conjugate isolated from the conjugation reaction mixture with a purity of higher than 96%, was characterized by: 1) slab-sodium dodecyl sulfate-polyacrylamide gel electrophoresis (SDS-PAGE) with specific stains for apparent molecular mass, purity, and the presence of reactants (IFN-α2b, $PEG_{2,40K}$) or conjugates; 2) ion-exchange chromatography (IEC) packed with Fractogel EMD COO⁻ 650 (S) for relative binding strength and purification; 3) strong-cation exchange-high performance liquid chromatography (HPLC) for heterogeneity; 4) bicinchoninic acid (BCA) protein assay for interferon content; 5) enzyme-linked immunosorbent assay (ELISA) for measuring the recognition ability of $PEG_{2,40K}$-IFN-α2b by monoclonal antibodies (mAbs) anti-IFN-α2b; and 6) *in vitro* bioassays for the effect of PEGylation on IFN-induced (antiviral/antiproliferative) activities. Using both thermal stability at 60°C and tryptic digestion, we also verified the protective effect of the $PEG_{2,40K}$ moiety on the *in vitro* stability of IFN-α2b in the conjugate. Finally, a pharmacokinetics study using rats was carried out to further characterize (*in vivo* stability) the $PEG_{2,40K}$-IFN-α2b conjugate.

MATERIALS AND METHODS

Materials

Clinical grade recombinant IFN-α2b, anti-recombinant IFN-α2b CBIFNA2.3 mAb, and anti-recombinant IFN-α2b CBIFNA2.4-HRP conjugate were commercial products supplied by CIGB (Center for Genetic Engineering and Biotechnology, Havana, Cuba). A branched 40K *N*-hydroxysuccinimide ester of PEG was purchased from Shearwater Polymers, a subsidiary of Nektar Therapeutics (San Carlos, CA, USA). Male Sprague–Dawley rats (150–200 g) were from the National Center for Laboratory Animal Production (Havana City, Cuba). The 96-well microtiter plates (Maxisorb) were from Nunc (Roskilde, Denmark). An SP-5PW HPLC column was obtained from TOSOH Biosep (Tokyo, Japan). Sequencing-grade trypsin for peptide mapping was purchased from Promega (Madison, WI, USA) and trypsin (1:250) for proteolytic degradation was from GIBCO BRL (Rockville, MD, USA). Fractogel® EMD COO⁻ 650 (S) and other reagents used were supplied by Merck (Darmstadt, Germany).

$PEG_{2,40K}$-IFN-α2b

Conjugation Reaction

IFN-α2b at 5 mg/ml, in 100 mM phosphate buffer (pH 6.5, 7, or 8) or in 50 mM sodium borate buffer (pH 8 or 9), was mixed with the activated $PEG_{2,40K}$ (solid or dissolved at 66 or 100 mg/ml in 1 mM HCl) at a molar ratio of 1:3. The conjugation reaction mixture (12 ml) was stirred for 2 h at 4°C. Diluted 50-fold, the reaction was stopped with 10 mM ammonium acetate buffer, pH 4.5. This sample was immediately separated by ion-exchange chromatography or stored at –20°C until use.

Separation by Ion-Exchange Chromatography

The reaction mixture was applied to a column (XK-26/60, Amersham Biosciences Ltd., UK) packed with Fractogel EMD COO⁻ 650 (S). The chromatography matrix had been previously equilibrated with 10 mM ammonium acetate buffer, pH 4.5 (10 ml/min). Eluting the gel matrix with equilibration buffer gave fraction 1 (unreacted $PEG_{2,40K}$). Fractions 2 (polyPEGylated interferon), 3 ($PEG_{2,40K}$-IFN-α2b), and 4 (unconjugated IFN-α2b) sequentially eluted with 40 mM ammonium acetate buffer, pH 4.5, with either 20, 40, or 700 mM sodium chloride. Each fraction was analyzed by slab-SDS-PAGE and by colorimetric assays for PEG/protein ratio, as described later. The monoPEGylated eluate was concentrated to approximately 1 mg/ml in 20 mM sodium acetate, pH 5, containing 150 mM sodium chloride. After concentration, $PEG_{2,40K}$-IFN-α2b was filtered in a 0.2-μm filter and stored at 4°C until use.

Analytical Techniques

The following methods were used for characterizing either the PEGylation reaction or IEC-purified $PEG_{2,40K}$-IFN-α2b.

Slab-SDS-PAGE

Either gradient (4–17% acrylamide) or linear (8% or 15% acrylamide) type slab-SDS-PAGE was used (23). The gels were then stained for protein with Coomassie brilliant blue (CBB). The stained gels were analyzed densitometrically with a ScanJet 4c/T scanner (Hewlett Packard, Palo Alto, CA, USA) and Molecular Analyst software (Bio-Rad Laboratory, Hercules, CA, USA). Gel bands containing PEG moieties were stained as described by Kürfurst (24). The polyacrylamide gel was agitated in 0.1 M perchloric acid for 10 min, then 5% barium chloride with 0.1 N iodine/potassium iodide solutions were simultaneously added to the gel bath. Iodine excess was washed off with water, until the background was clear.

Heterogeneity Assay

A strong-cation exchange column (TOSOH-Biosep, Tokyo, Japan, SP-5PW, 13 µm particle size, 21.5 mm diameter, 15 cm length) was used to analyze the heterogeneity of monoPEGylated IFN-α2b with HPLC (Lachrom HPLC system with a D7000 interface, L-7100 pump and L-7450 diode array detector). Pre-equilibration was done with 3.7 mM sodium acetate at pH 4.3 (buffer A). The $PEG_{2,40K}$-IFN-α2b was loaded and the column washed with buffer A. IFN isoforms were separated using a pH gradient of from 4.3 to 6.4 (buffer B, 10 mM dibasic potassium phosphate) at a flow rate of 4 ml/min and detected at 226 nm.

Selected IEC fractions were desalted by using a Vydac RP-C4 (5 µm particle size, 2.1 mm diameter, 5 cm length) column. The desalted samples were dried in a vacuum concentrator (Concentrator 5301; Eppendorf AG, Hamburg, Germany), then dissolved at 5 µg/ml in 1% NH_4HCO_3 and digested with trypsin for 6 h at 37°C (enzyme-to-protein weight ratio of 1:40). The digested samples were analyzed with a Vydac RP-C18 analytical column (5 µm particle size, 2.1 mm diameter, 25 cm length). Elution was performed with a 1–60% linear acetonitrile gradient in 0.1% aqueous trifluoroacetic acid over 60 min on the same column. Digested samples (100 µl) were injected to the HPLC system and monitored at 226 nm.

Protein Content

Protein content was measured by the BCA method using BCA protein assay reagent kit (Pierce, Rockford, IL, USA).

PEG Content

PEG content was determined by mixing each sample containing $PEG_{2,40K}$ with one-half volume of 5% barium chloride in 1 M HCl and one-half volume of 0.1 N iodine/potassium iodide solutions (25). After 15 min, absorbance at 535 nm was read using a Spectronic Genesys 2 spectrophotometer (Spectronic Instruments, Rochester, NY, USA). The polymer content was determined using a PEG standard curve (2.5–40 µg).

Enzyme-Linked Immunosorbent Assay

Each well of the microtiter plate was coated with 1 µg of anti-recombinant IFN-α2b CBIFNA 2.3 mAb in 0.1 ml of coating buffer (0.05 M Na_2CO_3, 0.05 M Na_2HCO_3, pH 9.6) and incubated for 3 h at 37°C (26,27). The coated plate was washed twice with washing solution [10 mM sodium phosphate and 145 mM NaCl (PBS), pH 7.2, containing 0.05% (v/v) polysorbate 20]. Then, 100-µl diluted samples were added per well in assay buffer [PBS containing 0.5% (w/v) skim milk]. After incubation for 30 min at 37°C, the plate was washed five times with PBS/polysorbate 20. Then, 70 µl of the conjugated second antibody (anti-IFN-α2b CBIFNA 2.4 mAb), labeled with horseradish peroxidase and diluted 1:6000 (v/v) in the assay buffer, were added and incubated at 23°C for 1 h. The plate was washed eight times with PBS/polysorbate 20, and then incubated for 15 min at 23°C with 100 µl of the substrate solution. The substrate solution contained 0.1 M Na_2HPO_4, 0.048 M citric acid, pH 5.5, and 0.45 g of *o*-phenylenediamine/l plus 0.3 g of H_2O_2/L. The reaction was stopped by adding 50 µl of 2.5 M H_2SO_4. Absorbance at 492 nm was measured by using an ELISA-plate reader (SensIdent Scan; Merck, Darmstadt, Germany).

Antiviral Activity

Antiviral activity of IFN-α2b with or without $PEG_{2,40K}$ was assayed by inhibition of the cytopathic effect produced by Mengo virus with Hep-2 cells (ATCC No. CCL23) (28). IFN samples serially diluted 1:2 (v/v) in minimum essential medium containing 2% fetal calf serum and 40 µg/ml of gentamicin were mixed with cell monolayers in 96-well microtiter plates. The plates were then incubated at 37°C for 24 h, under 3% CO_2 and 95% humidity. After the virus was added (10^7 TCID), the plates were incubated until the cytopathic effect (90% cell lysis) was evident (approximately 18–20 h) in the virus control wells (without IFN-α2b). Staining the remaining cells with crystal violet measured the degree of cell destruction. A microplate reader (Tecnosuma, Havana, Cuba) was used to determine the cytopathic effect. The resulting data were transformed to a linear regression through a probit transformation with validated software. The unit of antiviral activity was defined as the reciprocal of the sample dilution that yields 50% protection of cells against the Mengo-induced cytopathic effect. The potency of each sample was expressed in IU compared to a secondary reference calibrated against the 69/19 International World Health Organization IFN-α2b standard.

Antiproliferative Activity

The *in vitro* antiproliferative activity of IFN-α2b measured the ability of the cytokine to inhibit the growth of Daudi cells. Cells in 96-well microtiter plates were incubated with IFN samples serially diluted (1:2, v/v) in RPMI 1640 medium with 10% fetal calf serum and 40 µg/ml of

gentamicin. The cells were incubated for 72 h at 37°C, 5% CO_2 and 95% humidity. Wells without IFN-α2b were used as a negative control. Twenty microliters of 3-(4,5-dimethylthiazol-2-yl)-2,5-diphenyltetrazolium bromide (5 μg/ml in water) were added to each well. After incubation for 4 h at 37°C, 100 μl of 2-butanol was added and the absorbance at 578 nm read as described above.

Stability Analysis

Thermal Stability

IFN-α2b, PEG$_{2,40K}$-IFN-α2b were each diluted to 500 μg/ml in phosphate saline buffer, pH 7.4. A portion (200 μl) was placed into borosilicate vials and then sealed with chlorobutyl stoppers and 13-mm flip-off aluminum seals. These were stored at 60°C. Densitometric analysis of Coomassie blue-stained gels was performed at time intervals of 0, 1, 3, 6, and 12 days of storage.

Tryptic Digestion

Forty microliters of IFN-α2b and PEG$_{2,40K}$-IFN-α2b at 400 μg/ml in 4% sodium bicarbonate, pH 8, were each mixed with 10 μl of trypsin dissolved at 160 μg/ml of buffer. The reaction mixture was incubated with agitation at 37°C. Ten microliters of trifluoroacetic acid was added to stop the tryptic reaction. Densitometric analysis of Coomassie blue-stained gels containing the mixtures that reacted for 10, 30, 60, 120, or 240 min was used to determine the ability of the PEG$_{2,40K}$ moiety to protect IFN against trypsin degradation.

Pharmacokinetics

Pharmacokinetics of both monoPEGylated and native IFN-α2b were studied using male rats (200 g mean weight, 8–10 weeks old, Sprague–Dawley strain). Animals were anesthetized with sodium pentobarbital (40 mg/kg body weight) before any invasive procedures were conducted. Two random groups with three animals per sampling time from either mono-PEGylated or native IFN-α2b treatment were used. They were injected with a single 125 μg protein/kg body weight bolus, at the dorsal vein of the penis.

Rats were housed individually in separate cages and maintained under controlled conditions before and during the experiment (i.e., room temperature at 25 ± 2°C; relative humidity of 65%; 12 h light/dark cycle). Access to food and water was provided *ad libitum*. All animal procedures were carried out under the approval of the Animal Care and Use Committee from CIGB (Havana, Cuba) and conducted in accordance with the standard operating procedures for good laboratory practices in animal use, established at CIGB.

Blood samples of about 500 μl per animal were taken, by a retro-orbital puncture, before injection (pre-dose) and 0.083, 0.25, 0.5, 1, 3, 6, 12, 24, 48, and 72 h following the injections (post-dose). After collection at room temperature, all the blood samples were centrifuged at 4°C for 10 min. Then, serum was separated and stored frozen at –20°C until assayed.

The serum samples for measuring either native or monoPEGylated IFN-α2b were used in the ELISA assay described earlier. Data points were plotted as the means ± standard deviations from three animals per sampling time. The calculated mean serum drug concentration data were then fitted to poly-exponential equations. Interpretation was based on a classical compartment mammillary model, first-order elimination, using WinNonlin professional software (Version 2.1, Pharsight Inc., 1997, NC, USA) and following the Levenberg-Hartley modified Gauss-Newton minimization method. Different exponential models were tested to select the most suitable according to the AKAIKE information criterion (29). The resulting average pharmacokinetic parameters (±SEM; CV%) were calculated with standard procedures (30).

Statistical Analysis

All statistical analyses were performed using the GraphPad software (San Diego, CA, USA). Details of the data analysis and curve-fitting models used are explained in GraphPad Prism 4 user's guide (31).

RESULTS AND DISCUSSION

Synthesis of the PEG$_{2,40K}$-IFN-α2b Conjugate

Conjugation Reaction

The chemical reaction for the synthesis of PEGylated IFN-α2b is shown in Fig. 1. The PEG$_{2,40K}$-IFN-α2b is
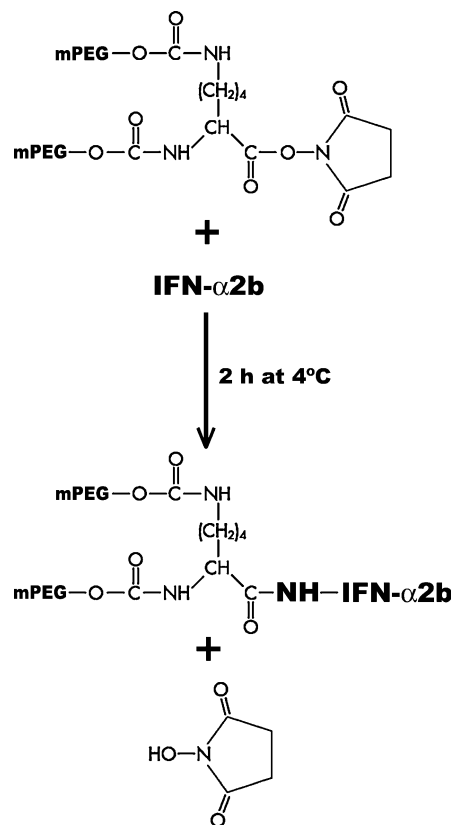
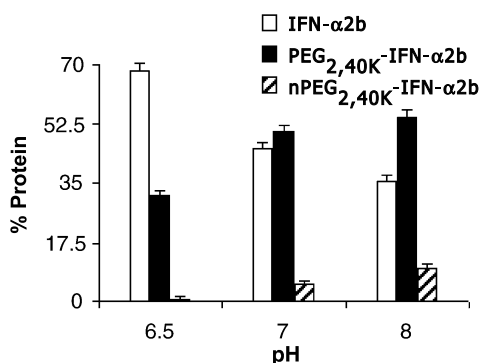**Fig. 1.** General scheme of the reaction to synthesize PEG$_{2,40K}$-IFN-α2b. Free amino groups of IFN-α2b react with PEG$_{2,40K}$ to form an amide bond between both macromolecules.
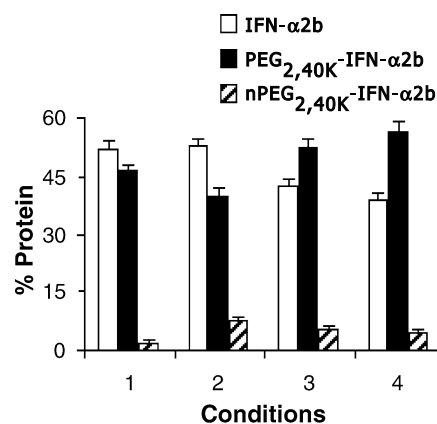
obtained when the *N*-hydroxysuccinimide ester of a 40K branched PEG reacts with free amino groups from IFN-α2b to form amide linkages between both macromolecules (11). This type of reaction should give a variety of other molecular species (oligomers) involving IFN-α2b and $PEG_{2,40K}$ together with unreacted protein and excess PEG polymer. PEGylation should occur by the electrophilic attack of the PEG carboxylic carbon on susceptible sites of IFN-α2b. Important sites are free amino groups of lysines, imidazolyl nitrogens of histidines, and the α-amino group at N-terminal cysteine. Coupling between $PEG_{2,40K}$ and free hydroxyl groups of IFN-α2b might also form an ester linkage (16).

We studied the PEGylation reaction at three different pH values (Fig. 2). The percentage of the IFN-α2b conjugate in its monomer state was increased from 31% at pH 6.5 to 55% at pH 8. At both pH 7 and 8, more than 35% of IFN-α2b remained in its native form. An appreciable amount (above 8%) of biPEGylated IFN was also formed. This reaction did not go to completion, even at a protein/PEG molar ratio of 1:2. One explanation may be that the activated $PEG_{2,40K}$ rapidly hydrolyzes in aqueous solutions. These results are similar to others that involved protein PEGylation at different pH values (32). Under defined experimental conditions (IFN-α2a at 5 mg/ml in 50 mM sodium borate buffer, pH 9, protein/$PEG_{2,40K}$ molar ratio of 1:3, reaction time of 2 h, temperature of 4°C), Bailon *et al.* (11) found a mixture of monomers (45–50%), oligomers (5–10%, predominantly dimer), and unmodified IFN-α2a (40–50%).

The yield of PEGylation may be in how a protein and the reacting PEG are mixed (33). We tried the addition of the $PEG_{2,40K}$ reagent in either solid state or solution. The IFN solution (10 ml) was buffered to pH 9 because activated $PEG_{2,40K}$ had to be dissolved in 1 mM HCl (2 ml). The results are shown in Fig. 3. The use of $PEG_{2,40K}$ in solution gave more monoPEGylated IFN-α2b (52% and 56% with $PEG_{2,40K}$ at 100 and 66 mg/ml, respectively) than it did when only added in its solid state. This might be explained by the time required for the two liquid kinetic phases to mix, which is shorter than is needed to dissolve the solid $PEG_{2,40K}$ reagent. It may be that a greater amount of activated $PEG_{2,40K}$ molecules thereby contact and react with the protein before

Fig. 3. PEGylation reaction using $PEG_{2,40K}$ in either solution or solid state. 1, The $PEG_{2,40\ K}$ reagent added to IFN-α2b was in its solid state and the pH was 8. 2, Same as in 1 except that the reaction pH was 9. 3, The $PEG_{2,40K}$ reagent added to the interferon dissolved at 100 mg/ml in 1 mM HCl solution with pH 9. 4, Same as in 3 except that the PEG was at 66 mg/ml. All the reactions were done with IFN-α2b at 5 mg/ml, in 50 mM borate buffer. The y-axis indicates the yields of each species as determined by densitometric analysis of Coomassie blue-stained proteins on slab-SDS-PAGE gels, done in duplicate.
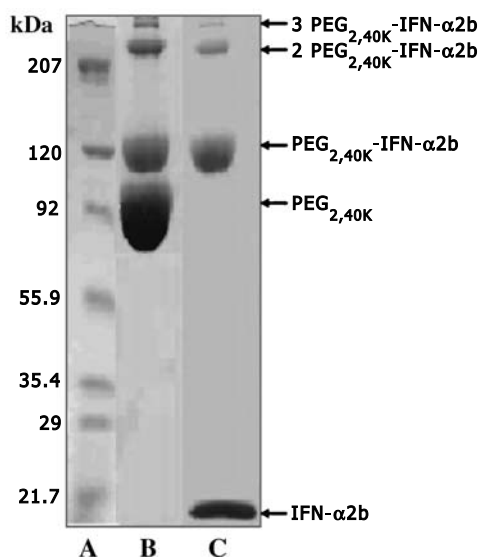
they are degraded by hydrolysis, favoring the conjugation reaction. Moreover, highly local $PEG_{2,40K}$ concentrations may not be generated that might lead to the formation of undesired oligomers.

Figure 3 shows that the amount (40%) of monoPEGylated IFN-α2b obtained at pH 9 is less than that obtained (47%) at pH 8. Since at pH 9 more biPEGylated IFN-α2b is obtained (1% *vs.* 8%), it seems that PEGylation yield increases with pH. At a higher pH, the proportion of groups susceptible to electrophilic attack may promote the PEGylation reaction (34).

Characterization by Slab-SDS-PAGE Separation of $PEG_{2,40\ K}$-IFN-α2b in the Reaction Mixture

The theoretical molecular mass of the monoPEGylated IFN-α2b is approximately 59,200 upon the basis of the 40,000 M_r for the branched PEG moiety and 19,200 M_r for IFN-α2b. In slab-SDS-PAGE the $PEG_{2,40K}$-IFN-α2b conjugate should migrate with a higher apparent molecular mass (approximately 120 kDa) than the actual, M_r (11). This increase in apparent molecular mass of the IFN conjugate is due to the contribution of the hydrated PEG moiety to its hydrodynamic radius (35).

Figure 4 shows the slab-SDS-PAGE profile of the macromolecule mixture obtained in a PEGylation reaction. The gel was stained by two methods: Coomassie brilliant blue (CBB, for proteins) (36) and iodine (I_2, for PEG) (24). The gel band that appears in the CBB-stained gel (lane C) below the 21,700 molecular mass standard band is unreacted IFN-α2b. This CBB band did not stain with iodine (lane B), as expected. The I_2-stained band (Fig. 4, lane B), with a mobility approximately matching that of the 92,000 molecular mass standard (Fig. 4, lane A), corresponds to unreacted PEG. This apparent molecular mass is similar to that described by other investigators (11). The bands (lanes B

Fig. 2. PEGylation reaction at different pH values. The reaction was performed in 100 mM sodium phosphate buffer. $PEG_{2,40K}$ solid reagent was added to the IFN-α2b solution (5 mg/ml) at a 2:1 molar ratio. The yields of each species (y-axis) were determined by densitometric analysis of Coomassie blue-stained proteins separated in slab-SDS-PAGE gels. Experiments were done in duplicate. Details are given in Materials and Methods.

Fig. 4. Slab-SDS-PAGE profile of PEGylation reaction. IFN-α2b (5 mg/ml) in 50 mM borate buffer, pH 9, was mixed with a twofold molar excess of $PEG_{2,40K}$ and left under agitation for 2 h at 4°C. The electrophoresis was conducted under reducing conditions in a gradient gel (4–17%). Lanes: (A) molecular mass marker, (B) reaction stained for PEG with iodine, (C) reaction stained with Coomassie brilliant blue R-250.
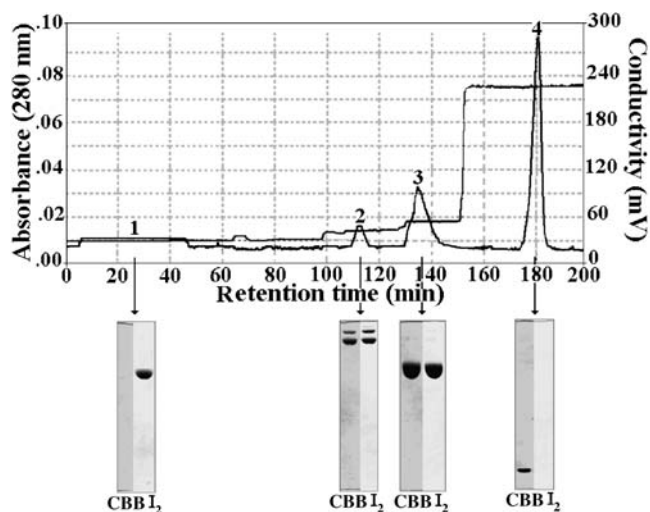

Fig. 5. Ion-exchange chromatography profile of PEGylation reaction. Fractogel[®] EMD COO⁻ 650 (S) chromatography was used to separate the PEGylation reaction mixture with a stepwise gradient (20, 40, and 700 mM NaCl) in 40 mM ammonium acetate, pH 4.5. The eluted fractions were analyzed using slab-SDS-PAGE (4–17% gradient gel) and specific staining for protein (CBB) and PEG (I_2). Fraction 1 eluted during the loading of the reaction mixture onto the column. The composition of each fraction is shown in Table I.

and C) detected by both staining methods corresponded to IFN conjugates of a different degree of substitution, as indicated in Fig. 4.

Isolation by Ion-Exchange Chromatography of $PEG_{2,40K}$-IFN-α2b and Further Characterization

IEC Separability

The neutral charge of PEG polymer precludes its separation with ion-exchange resins. Therefore, PEGylated proteins are expected to be bound less tightly in these types of chromatography gels than their native (unmodified) counterparts. The interaction strength between a PEGylated protein and an ion-exchange matrix is inversely proportional to the number of PEG chains attached per protein molecule (37).

Ion-exchange chromatography with Fractogel[®] EMD COO⁻ 650 (S) cation-exchange resin will separate IFN-α2a conjugates by charge difference (e.g., PEG-induced changes in the protein isoelectric point), which fractionates conjugates into their various molecular masses (33). Using this type of IEC, our PEGylation reaction mixture was separated into four fractions (Fig. 5). Follow-up slab-SDS-PAGE analysis revealed the species present in each fraction (Fig. 5); the content of IFN-α2b and $PEG_{2,40K}$ was estimated by colorimetric assays (Table I). The monoPEGylated IFN-α2b eluted in fraction 3, with a lower concentration (40 mM NaCl) than necessary to elute unmodified protein (fraction 4, 700 mM NaCl), and higher than required to elute the oligomers (fraction 2, 20 mM NaCl) and excess PEG (fraction 1). Compared to unreacted IFN-α2b, the $PEG_{2,40K}$-IFN-α2b interacted less strongly with the ion-exchange matrix because of the presence of the PEG moiety in its structure. The

same phenomenon explains why the mono-PEGylated conjugate interacted with the matrix more strongly than both the other PEGylated derivatives having more than one $PEG_{2,40K}$ chain per protein monomer and the unreacted protein-free PEG.

The chromatographic process used in this study also demonstrated its utility in purifying the $PEG_{2,40K}$-IFN-α2b with more than 96% purity (Fig. 6). The IEC-purified $PEG_{2,40K}$-IFN-α2b accounted for about 86.7 ± 7% (n = 3) of the total 28 mg of the chromatographed conjugate.

Heterogeneity of the MonoPEGylated IFN-2b

The reaction between the activated $PEG_{2,40K}$ and IFN can occur at several possible protein sites. In IFN-α2b, these are the amino groups of its 10 lysines, the α-amino group at the N-terminal cysteine, the imidazolyl nitrogens of its 3 histidines, and the hydroxyl groups at its 14 serines, 10 threonines, and 5 tyrosines. Various factors, including inherent nucleophilicity, solvation, protein conformation, as well as local electronic and pK_a effects will determine the

Table I. Molar Ratios (Protein:$PEG_{2,40K}$) Found in IEC (Fractogel[®] EMD COO⁻)—Separated Fractions

Fraction	Ratio of Protein/$PEG_{2,40K}$	Proposed Composition
1	0:1	Excess $PEG_{2,40K}$ reagent
2	1:1.03 (±0.15)	MonoPEGylated IFN-α2b
3	1:2.16 (±0.21)	PolyPEGylated IFN-α2b
4	1:0	Unmodified IFN-α2b

A specific colorimetric assay, as described under Materials and Methods, was used to determine the protein or $PEG_{2,40K}$ content in each fraction.
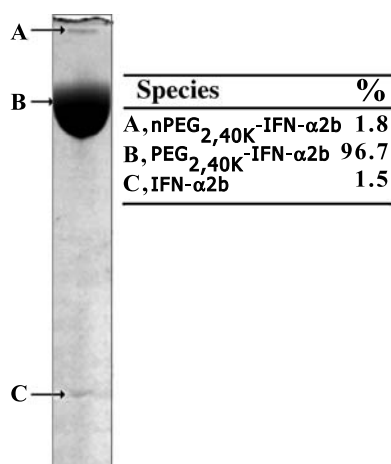
Fig. 6. Analysis of $PEG_{2,40K}$-IFN-α2b purity. Slab-SDS-PAGE (4–17% gradient gel) to analyze the monoPEGylated IFN-α2b purified by Fractogel® EMD COO⁻ 650 (S) chromatography. The proportion of each species was determined by densitometric analysis of duplicate Coomassie blue-stained gels.

actual reactivity of the potential PEGylation sites. The resulting monoPEGylated IFN-α2b will probably be composed of a heterogeneous population of different positional isomers (38).

The purified $PEG_{2,40K}$-IFN-α2b obtained was analyzed by ion-exchange chromatography in a SP-5PW column (Fig. 7). The conjugated IFN, which migrated as a single band in slab-SDS-PAGE (Fig. 6), was now separated into eight fractions with different retention times. The chromatographic profiles of three independent preparation batches were very similar (Fig. 7A, B, C), again indicating that the PEGylation process is reproducible (7).

This is consistent with previous work relating to the heterogeneity of PEGylated IFN (11,39). The IEC separation profile of $PEG_{2,40K}$-IFN-α2a displays only two peaks with baseline separation, and another six with partial separation (39). Using a combination of cation-exchange HPLC, peptide mapping, amino acid sequencing, and mass spectrometric analyses, Bailon *et al.* (11) determined that the exact cause for the heterogeneity of PEGylated IFN is that a single unit of $PEG_{2,40K}$ randomly attaches one unit of either Lys^{31}, Lys^{121}, Lys^{131}, or Lys^{134}, from IFN-α2a. Approximately 94% of the PEG attachment takes place in these four sites and the remaining 6% of the PEGylation occurs at Lys^{70} and Lys^{83}. More recently, Foser *et al.* found that out of 11 potential sites for PEGylation, 9 (Lys^{31}, Lys^{49}, Lys^{70}, Lys^{80}, Lys^{112}, Lys^{121}, Lys^{131}, Lys^{134}, and Lys^{164}) are detectable (5–10% for each isomer) by strong-cation exchange chromatography (39).

We carried out peptide mapping with trypsin digestion to confirm that different positional isomers of IFN-α2b conjugate exist in each IEC-separated fraction. We chose to use trypsin because this protease specifically cleaves IFN-α2b at the carboxylic side of lysine and arginine residue, and lysine is expected to be one of the most probable sites of PEGylation in our IFN (11). The hydrolysis of peptide bonds does not occur when the lysines are PEGylated. This is why different positional isomers might be expected to produce different peptide maps (35,38).

The tryptic digestion maps of three selected IEC-separated fractions (peaks 2, 4, and 5 in Fig. 7) were monitored using RP-HPLC (Fig. 8). The fact that there were differences from one to another in terms of peak intensity (marked with arrows in Fig. 8) suggests that distinct positional isomers of the IFN-α2b conjugate are present in the isolated fractions. None of the digestion maps illustrated in Fig. 8 is able to show the total elimination of any of the PEG-related peaks. We think this might be caused by the incomplete IEC separation of positional isomers, something known to be a very complicated problem (38). Even so, PEGylation with the large, branched $PEG_{2,40K}$ moiety seems to result into a product less heterogeneous compared with PEG-based IFN conjugates that contain small, linear PEG chains. Conjugation with the lower molecular mass 12,000 PEG polymer (at pH 6.5) was less selective for the individual lysines, with about 48% of the species linked to His^{34} residue
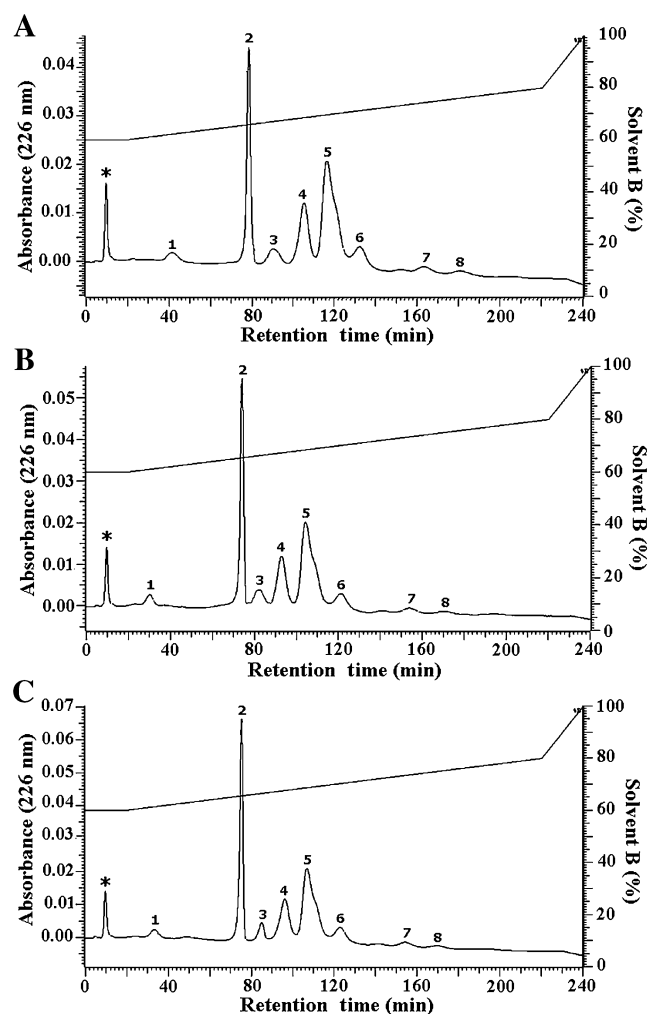
Fig. 7. Heterogeneity analysis of three independent batches (A, B, and C) of $PEG_{2,40K}$-IFN-α2b. Samples (1 ml of the IFN conjugate at 1 mg/ml diluted 10-fold in buffer A) were applied to a strong cation-exchange column (SP-5PW) equilibrated with 40% of 3.7 mM sodium acetate, pH 4.3 (buffer A) and 60% of 10 mM potassium phosphate dibasic, pH 6.4 (buffer B). The separation was performed with a linear gradient from 60% to 80% of buffer B in 200 min. The peak marked with an asterisk in the figure indicates the solvent front.
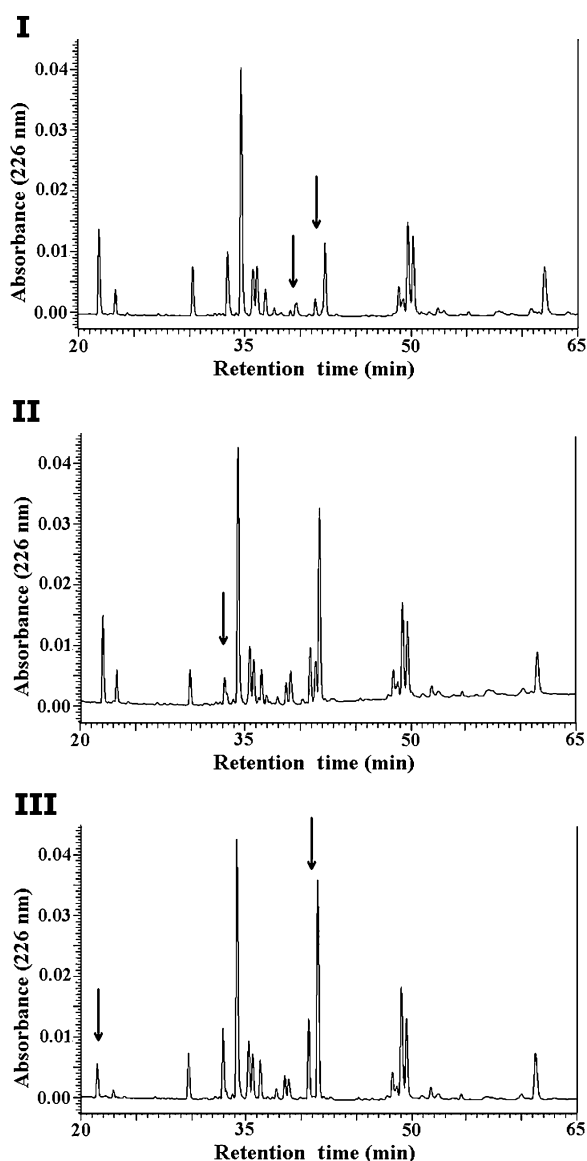
Fig. 8. Peptide mapping of different fractions (2, 4, and 5 in Fig. 7) on strong cation-exchange chromatography-separated PEG$_{2,40K}$-IFN-α2b. The fractions were digested (4 h, 37°C) with trypsin (weight ratio of 1:40) and the mixture applied directly to a C18 RP-HPLC-column. Peptides were eluted with a linear gradient of 20–65% acetonitrile (with 0.1% of trifluoroacetic acid) in water. Arrows indicate where major differences were observed between the peptide maps.

(4,7). The remaining 13 different IFN species were found to be PEGylated at various lysines, the *N*-terminal cysteine, as well as serine, tyrosine, and another histidine residue (4). Also, the conjugation of IFN-α2a using PEG$_{5K}$ was a mixture of 11 different monoPEGylated isomers (38). The exact location of the amino acid sites of PEGylation and the proportion of each positional isomer in these mixtures remain undetermined.

Detectability of PEG$_{2,40K}$-IFN-2b by the BCA Method

The reaction of protein with alkaline Cu^{2+}, known as the biuret reaction, produces cuprous ion (Cu^+). Two separate sources are associated with the formation of Cu^+ (40,41): 1) oxidation of cysteine, tyrosine, and tryptophan residues and 2) temperature-dependent reaction of peptide bonds with Cu^{2+}. Reaction of this Cu^+ with a water-soluble sodium salt of bicinchoninic acid forms an intense, stable purple complex that develops proportionally over a broad range of protein concentrations. The BCA assay has been used to measure down to 2 μg/ml of protein solutions.

To determine whether the PEG$_{2,40K}$ chain moiety affects the interaction between Cu^{2+} and the peptide bonds from PEGylated IFN, we used BCA with the native IFN-α2b or PEG$_{2,40K}$-IFN-α2b samples (Fig. 9). Both the native and monoPEGylated IFN-α2b groups by BCA showed comparable dose–response curves (variable slope). This curve, with an r^2 of 0.9979, was selected because the concentration range (0.0001–200 μg/ml) studied was broader than the linear concentration range (2–20 μg/ml) for the BCA method. The PEG$_{2,40K}$ worked well with BCA and we concluded, therefore, that IFN-α2b in its monoPEGylated conjugate is detectable and quantifiable by BCA.

In Vitro Biological Activity

Coupling of PEG chains to a therapeutic protein generally affects some of its *in vitro* biological activities (42). This may have two major causes: 1) PEG-related steric impediments that disturb protein–receptor interactions and 2) certain topological changes occurring in the structure of the conjugated protein that diminish the accessibility of the protein to its receptor binding sites. The end result is that the binding affinity of PEG-based protein conjugates is lowered. The magnitude of this problem depends on the size, structure, and number of PEG chains that are bound to the PEGylated protein (43).

Table II (column and row 3) shows the *in vitro* antiviral activity of four independent batches of purified PEG$_{2,40K}$-IFN-α2b. The antiviral activities of two other IEC-separated fractions (2 and 4 in Fig. 5), the unseparated conjugation mixture, and the initial IFN-α2b are given (Table II, column 3). MonoPEGylated IFN-α2b showed an antiviral specific activity of about 2% of the initial IFN-α2b. This value, although low, is not far from the IFN activities of other authors. For example, Bailon *et al.* described that one of their
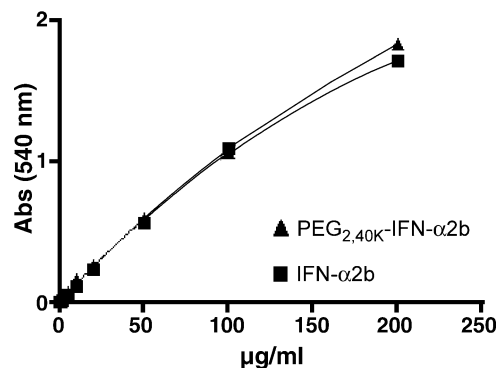
Fig. 9. Detectability of PEG$_{2,40K}$-IFN-α2b by the BCA method was carried out to assay samples of both species (native and conjugate IFN-α2b). The points in the graph represent the plotting of the absorbance values at 540 nm (y-axis) against the concentration values (x-axis, samples in triplicate).

Table II. *In Vitro* Specific Biological Activities of Reaction Fractions Separated by Ion-Exchange Chromatography (Fractogel$^{®}$ EMD COO$^-$)^a

	Batch	Antiviral Activity (IU/mg)	Antiproliferative Activity (IU/mg)
PolyPEGylated IFN-α2b		$1.7 \times 10^4 \pm 8.5 \times 10^3$	$1.9 \times 10^4 \pm 9.5 \times 10^3$
MonoPEGylated IFN-α2b	1	$2.8 \times 10^6 \pm 1.4 \times 10^6$	$3.1 \times 10^6 \pm 1.6 \times 10^6$
	2	$3.1 \times 10^6 \pm 1.6 \times 10^6$	–
	3	$2.3 \times 10^6 \pm 1.2 \times 10^6$	–
	4	$2.4 \times 10^6 \pm 1.2 \times 10^6$	–
Unmodified IFN-α2b		$1.6 \times 10^8 \pm 8.0 \times 10^7$	$1.5 \times 10^8 \pm 7.5 \times 10^7$
Reaction mixture		$1.5 \times 10^8 \pm 7.5 \times 10^7$	–
Initial IFN-α2b		$1.3 \times 10^8 \pm 6.5 \times 10^7$	–

^{a} For comparison the bioactivities of the initial native IFN-2b and unseparated reaction mixture are shown in the table.

$PEG_{2,40K}$-IFN-α2a preparations had a relative antiviral specific activity of only 7% of the starting IFN (11). Reduced *in vitro* antiviral activity has also been observed with PEG_{12K}-IFN-α2b (7).

An *in vitro* antiproliferative assay followed the same pattern as the antiviral assay (Table II). This may be explained by the effect on the linked, large (40K) PEG chains on the IFN-α2b–receptor interaction, thereby reducing biological activity.

Even when both the antiviral and antiproliferative activities of the PEGylated IFN species appear to be lower than that of the initial IFN-α2b, it is likely [Bailon *et al.* with IFN-α2a (11)] that the relatively short incubation time (hours) of the *in vitro* assays used is not enough for $PEG_{2,40K}$-IFN-α2b to demonstrate maximum effectiveness. Nevertheless, this phenomenon is not predictive of *in vivo* protein bioactivities. PEGylation interference in receptor binding should be compensated by a result in biological effect with the extended exposure time from the larger *in vivo* half-life of the $PEG_{2,40K}$-IFN-α2b. This is supported by other work in which 1) PEG_{12K}-IFN-α2b was found to be as therapeutically effective (e.g., in terms of both *in vitro* antiviral activity and cell-mediated immune responsiveness) as the parent cytokine (15) and 2) $PEG_{2,40K}$-IFN-α2a having only 5–10% of the original *in vitro* antiviral activity of IFN-α2a was more effective (e.g., 69% *vs.* 29% in terms of virological response) in treating patients infected with hepatitis C virus than standard IFN (11).

On the other hand, a Kruskal-Wallis test applied to analyze the *in vitro* antiviral activity values of four independent batches of $PEG_{2,40K}$-IFN-α2b showed that there was no significant difference (p < 0.05) between them, suggesting the present process involving multiple conjugation–purification steps is reproducible. The difference between the biological activities of the native IFN-α2b used for conjugation reaction and the IEC-purified unreacted IFN was found to be in the range of assay variation (± 50%). This indicates that the present process for $PEG_{2,40K}$-IFN-α2b does not affect the integrity of the protein, and that the biological activity changes are related only to the presence of the $PEG_{2,40K}$ moiety in the conjugate.

Identification of $PEG_{2,40K}$-IFN-2b by ELISA with Specific mAbs for IFN-2b

IFN-α2b is recognized by the mAbs IFN-α2bCBIFNA2.3 and IFN-α2bCBIFNA2.4 (27). The CBIFNA2.3 mAb tightly binds, and, *in vitro*, neutralizes the Mengo virus biological activity of IFN-α2b, while the CBIFNA2.4 mAb has a high affinity for solid phase-adsorbed IFN-α2b. The CBIFNA2.4 mAb does not compete with the CBIFNA2.3 mAb. These IgG$_1$-subclass mAbs recognize conformational epitopes of IFN-α2b, which are exposed when the cytokine is correctly folded. A previously developed ELISA assay based on these mAbs accurately quantifies biologically active IFN-α2b even in the presence of *Escherichia coli*-derived protein mixtures, while at the same time discriminating from incorrectly folded IFN-α2b molecular species from disulfide-bonded species (27). Consequently, this ELISA not only measures low concentrations (down to 0.2 ng/ml) of IFN-α2b, but may also show IFN integrity and has been used in the process and quality control of large-scale production of IFN-α2b (27).

To know if our PEGylation process influences the recognition of IFN-α2b by specific anti-IFN mAbs, we assayed either native IFN-α2b or $PEG_{2,40K}$-IFN-α2b samples by ELISA (Fig. 10). After side-by-side comparison, the resulting immunoreactivity data were adjusted to two dose–response curves with variable slope, and were significantly different (p < 0.0001). This allowed us to conclude that the attachment of $PEG_{2,40K}$ to IFN-α2b inhibits the binding of mAbs IFN-α2bCBIFNA2.3/IFN-α2bCBIFNA2.4 to the IFN moiety in the conjugate. This decrease in immunoreactivity may be due to: 1) conformational changes of the cytokines
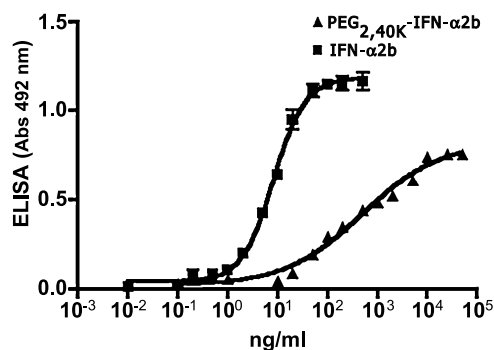
Fig. 10. Recognition of $PEG_{2,40K}$-IFN-α2b by ELISA with specific mAbs anti-IFN-α2b. Increasing amounts of either native or conjugate IFN-α2b species were assayed by ELISA, as described under Materials and Methods. The points in the graphs were fitted to a four parameter logistic function by nonlinear regression using the GraphPad Software (San Diego, CA, USA).

that may occur on PEGylation of IFN-α2b and might directly influence the IFN–mAbs interaction, 2) a PEG-related steric hindrance of the cytokine for these specific mAbs, or 3) the combination of both phenomena. Previously, the conjugation of a linear 12,000 PEG to IFN-α2b affected neither the protein secondary structure as analyzed by circular dichroism nor its recognition by ELISA (7). Consequently, we believe that the second cause is the major factor inhibiting the recognition of this conjugated IFN-α2b.
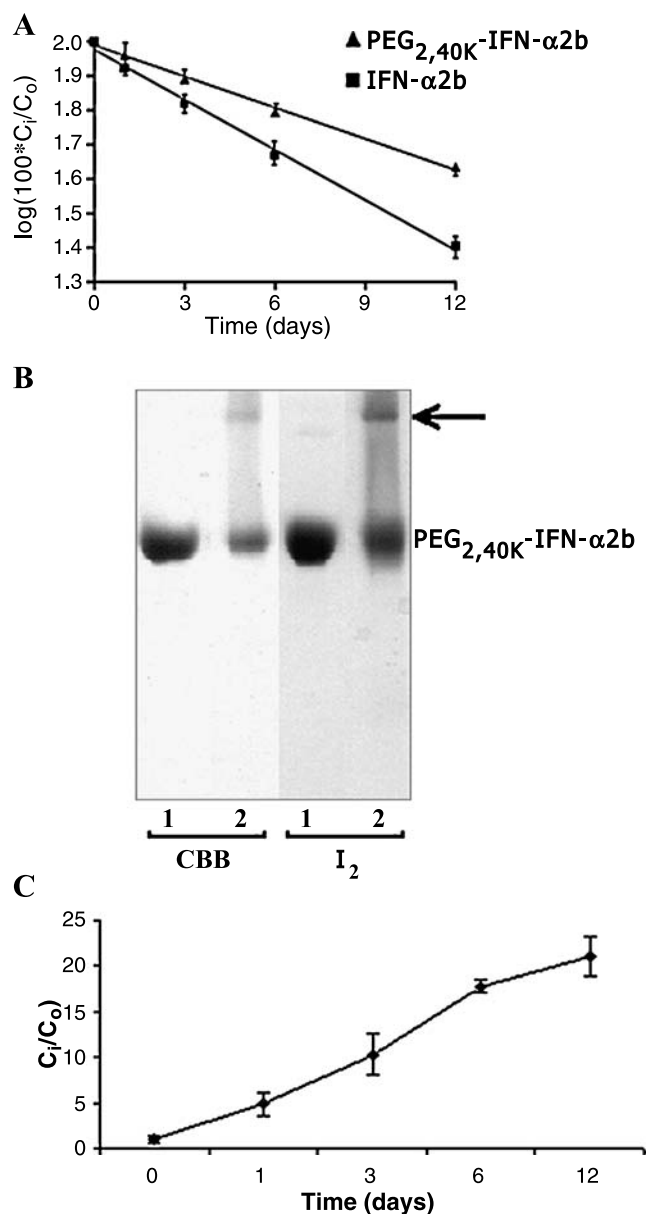
Table III. Kinetic Parameters of Thermal Stability of IFN-α2b and PEG$_{2,40\ K}$-IFN-α2b^a

Specie	$k \times 10^2$ (day^{-1})	$t_{1/2}$ (day)
IFN-α2b	4.85 ± 0.20	5.72
PEG$_{2,40K}$-IFN-α2b	3.02 ± 0.12	9.61

^{a} Samples in PBS at 500 μg/ml were dispensed into borosilicate glass vials and stored at 60°C. The residual relative concentration was evaluated by densitometric analysis of Coomassie blue-stained gels as described in the Materials and Methods section. The results are expressed as mean (n = 3) ± S.D.
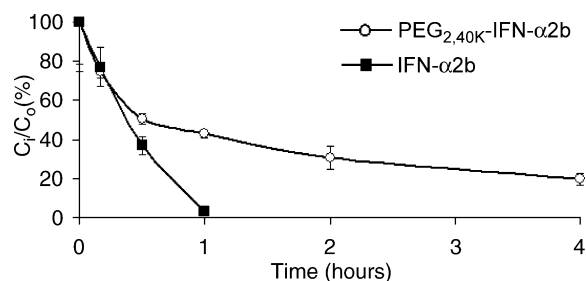
On the Stability of PEG$_{2,40K}$-IFN-α2b

Thermal Stability

PEGylation usually increases the thermal stability of proteins (43) by: 1) sterically blocking degradation pathways induced by hydrophobic interactions and 2) generating non-specific steric-hindrance of the intermolecular interactions that are involved in thermal instabilities (44).

We tested the ability of PEG$_{2,40K}$ to protect IFN-α2b against thermal degradation at 60°C. The decomposition kinetics of either PEG$_{2,40K}$-IFN-α2b or IFN-α2b does not follow a unimolecular rate-determining step. This may be a consequence of many interdependent protein decomposition pathways, as well as the general complexity of decomposition kinetics that may take place in aqueous solution. Nevertheless, to compare the difference in the stability of the native and conjugated IFN, we adjusted the thermal inactivation of IFN-α2b and PEG$_{2,40K}$-IFN-α2b, to a first-order kinetic model (Fig. 11A). Thus, the kinetics (k_{obs} and half-life) constants presented in Table III were calculated from linear relationships (r^2 of 99.5 for both species) between the logarithms of residual relative concentration from protein by densitometric analysis of slab-SDS-PAGE and time.

The difference between the specific rates of degradation for both biomolecules was found to be statistically significant (p = 0.00025). The half-life of PEG$_{2,40K}$-IFN-α2b was 1.7-fold greater than that of unPEGylated IFN. Although the mechanism responsible for the thermal degradation of

Fig. 11. Thermal stability of IFN-α2b and PEG$_{2,40K}$-IFN-α2b. Samples in borosilicate glass vials were stored at 60°C. (A) The y-axis indicates the ratio of interferon concentration over time with respect to its initial concentration (t = 0). (B) Slab-SDS-PAGE (gradient gel 4–17%) analysis of PEG$_{2,40K}$-IFN-α2b at days 0 (1) and 12 (2). The gels were stained with Comassie blue (CBB) or iodine (I$_2$). Arrow indicates a higher-molecular-mass-band. (C) The y-axis indicates the relative concentration of the emerging band (arrow in B). The C$_i$/C$_o$ parameter was determined by densitometric analysis of Coomassie blue-stained gels.

Fig. 12. Resistance of PEG$_{2,40K}$-IFN-α2b to tryptic degradation. PEGylated or native (control) interferon samples were incubated with trypsin, at a trypsin to protein weight ratio of 1:10. The reaction was left to occur at 37°C under agitation for the indicated times. Adding trifluoroacetic acid stopped the reaction. Ci/Co in the y-axis indicates the concentration of remaining IFN-α2b at each reaction time, with respect to the interferon concentration in t = 0. The concentration of interferon (PEGylated or not) was estimated by densitometric analysis of Coomassie blue-stained gels.

Table IV. Summary of Both PEGylated and Native IFN-α2b Pharmacokinetic Parameters, in Male Sprague–Dawley Rats, After Single 125 μg/kg Intravenous Dose

Parameter[a]	IFN-α2b			PEG$_{2,40K}$-IFN-α2b			
	Estimated	± SEM	CV%	Estimated	± SEM	CV%	p-value
AUC (μg·h/ml)	$6.3 \cdot 10^{-5}$	$7 \cdot 10^{-6}$	10.4	0.22	0.08	36.7	0.009
t½ (h)	0.07	0.02	28.8	23.1	10.3	44.7	0.030
CL (L/h)	397.5	41.3	10.4	0.11	0.04	36.7	0.001
Vss (L)	43.7	1.2	2.8	8.6	1.5	17.4	0.009
MRT (h)	0.11	0.03	28.8	77.9	38.0	48.7	0.045

[a] AUC, area under drug concentration *vs.* time curve; CL, systemic clearance; MRT, mean residence time; t½ elimination half-life; Vss, volume of distribution at steady state.

PEG$_{2,40K}$-IFN-α2b is not known, it is certainly associated with the formation of IFN species of higher molecular mass than the intact conjugate (Fig. 11B). The species indicated by an arrow in Fig. 11B may have been produced by aggregation, and also markedly increased with time (Fig. 11C).

Our results confirm the results of others (44,45).

Resistance to Tryptic Degradation

One of the reasons for the long-term stability of PEGylated proteins circulating *in vivo* might be their resistance to proteinase-induced degradation (42). To verify that IFN-α2b had enhanced resistance to proteolysis, we carried out an *in vitro* experiment in which both PEGylated and native (control) IFN were digested with trypsin. The PEG$_{2,40K}$-IFN-α2b showed more resistance to tryptic digestion than the native IFN (Fig. 12). A similar effect against protease digestion is known with PEGylated proteins other than IFN-α2b (e.g., tumor necrosis factor, epidermal growth factor) (46,47).

Pharmacokinetic Analysis

PEGylation prolongs the residence time of protein drugs in the body. In particular, PEG-based conjugates of IFN-α have been shown to possess an elimination half-life in humans greater than that corresponding to the non-PEGylated cytokine (3–8 h *vs.* 54 h for both PEG$_{5K}$-IFN-α2a and PEG$_{12K}$-IFN-α2b or 65 h for PEG$_{2,40K}$-IFN-α2a) (5).

Here, pharmacokinetic parameters of both monoPEGylated and native IFN-α2b were compared after single intravenous bolus injections into male Sprague–Dawley rats (Table IV). Figure 13 depicts the serum concentration time course corresponding to both macromolecules, and their predicted curve-fitting profiles obtained by nonlinear regression techniques. Peak drug concentrations were observed at the first sampling time point followed by an exponential decay. PEG$_{2,40K}$-IFN-α2b concentrations declined over time, whereas those for unconjugated IFN-α2b were closer to a monoexponential model. The level of the PEG$_{2,40K}$-IFN-α2b remaining in serum, detected in the rats up to 72 h after dosing, was considerably higher than that of the non-PEGylated IFN-α2b. In fact, from 6 h on, our ELISA did not find detectable levels of the unconjugated IFN-α2b (data not shown). Another effect of IFN-α2b PEGylation was to shorten the distribution volume parameter (Table IV). This

may be due to the detrimental contribution of the PEG moiety for distribution into peripheral tissues associated with gradient-driven transfer across cell membranes. Similar results were obtained with IFN-α2a PEGylated with the PEG$_{2,40K}$ reagent (5). The area under the curve for PEG$_{2,40K}$-IFN-α2b decays up to the last time point (72 h) was almost 3500-fold greater than for the native IFN-α2b (Table IV). Consequently, PEG$_{2,40K}$-IFN-α2b had a longer active life in rats.

Likewise, the PEG$_{2,40K}$ moiety had a 330-fold and 708-fold increase in elimination half-life (t½) and mean residence time (MRT) parameters (Table IV). This effect was due to the slower systemic clearance (p < 0.05) of the conjugate.
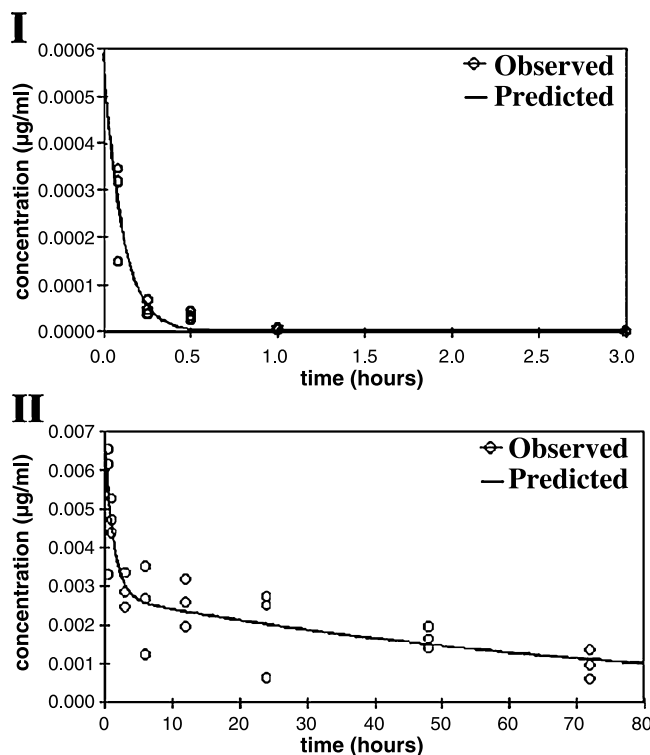
Fig. 13. IFN-α2b time course following a single 125 μg/kg intravenous bolus dose in male Sprague–Dawley rats. The symbols (open circles) represent the observed concentration data (three points per sampling time) from each treatment group (i.e., graph I for the unconjugated IFN; graph II for the PEG$_{2,40K}$-IFN-α2b). The continued lines represent the predicted values according to the best fitted-curve using compartment modeling.

Therefore, the rats treated with PEG$_{2,40K}$-IFN-α2b experienced a more prolonged exposure to IFN activity than those treated with unconjugated IFN-α2b. These results predict that a remarkable improvement in the sojourn of our IFN-α2b in the systemic circulation can be achieved by conjugating to PEG$_{2,40K}$.

CONCLUSION

IFN-α2b was conjugated with PEG$_{2,40K}$. The resulting monoPEGylated IFN-α2b product (approximately 56%) was accompanied by such other by-products as polyPEGylated IFN plus unconjugated reactants (IFN-α2b, PEG$_{2,40K}$). The reaction mixture was separable into four fractions by ion-exchange chromatography (Fractogel® EMD COO⁻ 650 [S]). The monoPEGylated conjugate was isolated (86.7 ± 7%) with a purity of 96% or higher. Both the *in vitro* antiviral and antiproliferative activity were lowered to about 2% of that of IFN-α2b, as expected. IFN-α2b in the monoPEGylated conjugate was detectable and measured by the BCA assay. However, the PEG$_{2,40K}$ moiety reduced the ability of the cytokine to be recognized by specific (CBIFNA2.3 and CBIFNA2.4) anti-IFN-α2b mAbs in an ELISA format. The heterogeneity of the monoPEGylated IFN-α2b shown by IEC-HPLC was thought to be due to the presence of different positional isomers in the separated fractions with this conjugate. The same level of heterogeneity was also obtained for different conjugation batches. PEGylation enhanced (1.7-fold) the thermal stability at 60°C of IFN-α2b. Also, the susceptibility to tryptic digestion of this conjugate was significantly diminished. Compared to IFN-α2b alone, the serum half-life of PEG$_{2,40K}$-IFN-α2b was augmented 330-fold. Further, a 708-fold increase in mean plasma residence time concomitant with sustained serum concentrations were shown. This study may be used as a reference point for scale-up and clinical applications.

REFERENCES

1. R. L. Cavalieri, E. A. Havell, J. Vilcek, and S. Pestka. Synthesis of human interferon by Xenopus laevis oocytes: two structural genes for interferons in human cells. *Proc. Natl. Acad. Sci. USA.* **74**:3287–3291 (1977).
2. S. Baron, S. K. Tyring, W. R. Fleischmann, D. H. Coppenhaver, D. W. Niesel, G. R. Klimpel, G. J. Stanton, and T. K. Hughes. The interferons. Mechanisms of action and clinical applications. *JAMA* **11**:1375–1383 (1991).
3. P. Lopez Saura. What is interferon good for? Ten years of experience in Cuba. *Biotecnol Apl* **9**:207–227 (1992).
4. Y. S. Wang, S. Youngster, M. Grace, J. Bausch, R. Bordens, and D. F. Wyss. Structural and biological characterization of pegylated recombinant interferon alpha-2b and its therapeutic implications. *Adv. Drug Deliv. Rev.* **54**:547–570 (2002).
5. K. Rajender Reddy, M. W. Modi, and S. Pedder. Use of peginterferon alfa-2a (40 KD) (Pegasys) for the treatment of hepatitis C. *Adv. Drug Deliv. Rev.* **54**:571–586 (2002).
6. R. J. Wills. Clinical pharmacokinetics of interferons. *Clin. Pharmacokinet.* **19**:390–399 (1990).
7. M. Grace, S. Youngster, G. Gitlin, W. Sydor, L. Xie, L. Westreich, S. Jacobs, D. Brassard, J. Bausch, and R. Bordens. Structural and biologic characterization of pegylated recombinant IFN-alpha2b. *J. Interferon Cytokine Res.* **21**:1103–1115 (2001).
8. A. Ahmed and E. B. Keeffe. Treatment strategies for chronic hepatitis C: update since the 1997 National Institutes of Health Consensus Development Conference. *J. Gastroenterol. Hepatol.* **14**(Suppl):S12–S18 (1999).
9. P. Kontsek, H. Liptakova, and E. Kontsekova. Immunogenicity of interferon-alpha 2 in therapy: structural and physiological aspects. *Acta Virol.* **43**:63–70 (1999).
10. C. Nalin and P. Rosen. U. S. Patent No. 5,382,657 (1995).
11. P. Bailon, A. Palleroni, C. A. Schaffer, C. L. Spence, W. J. Fung, J. E. Porter, G. K. Ehrlich, W. Pan, Z. X. Xu, M. W. Modi, A. Farid, W. Berthold, and M. Graves. Rational design of a potent, long-lasting form of interferon: a 40 kDa branched polyethylene glycol-conjugated interferon alpha-2a for the treatment of hepatitis C. *Bioconjug. Chem.* **12**:195–202 (2001).
12. K. A. Nieforth, R. Nadeau, I. H. Patel, and D. Mould. Use of an indirect pharmacodynamic stimulation model of MX protein induction to compare in vivo activity of interferon alfa-2a and a polyethylene glycol-modified derivative in healthy subjects. *Clin. Pharmacol. Ther.* **59**:636–646 (1996).
13. C. W. Gilbert and M. Park-Cho. U. S. Patent No. 5,651,974 (1997).
14. P. Glue, J. W. Fang, R. Rouzier-Panis, C. Raffanel, R. Sabo, S. K. Gupta, M. Salfi, and S. Jacobs. Pegylated interferon-alpha2b: pharmacokinetics, pharmacodynamics, safety, and preliminary efficacy data. Hepatitis C Intervention Therapy Group. *Clin. Pharmacol. Ther.* **68**:556–567 (2000).
15. K. L. Lindsay, C. Trepo, T. Heintges, M. L. Shiffman, S. C. Gordon, J. C. Hoefs, E. R. Schiff, Z. D. Goodman, M. Laughlin, R. Yao, and J. K. Albrecht. Hepatitis Interventional Therapy Group. A randomized double-blind trial comparing pegylated interferon α-2b to interferon α-2b as initial treatment for chronic hepatitis C. *Hepatology* **34**:395–403 (2001).
16. C. Monfardini, O. Schiavon, P. Caliceti, M. Morpurgo, J. M. Harris, and F. M. Veronese. A branched monomethoxypoly-(ethylene glycol) for protein modification. *Bioconjug. Chem.* **6**:62–69 (1995).
17. J. M. Harris, F. M. Veronese, P. Caliceti, and O. Schiavon, U. S. Patent No. 5,932,462 (1999).
18. I. L. Koumenis, Z. Shahrokh, S. Leong, V. Hsei, L. Deforge, and G. Zapata. Modulating pharmacokinetics of an anti-interleukin-8 F(ab′)(2) by amine-specific PEGylation with preserved bioactivity. *Int. J. Pharm.* **198**:83–95 (2000).
19. A. von Gabain, E. Lundgren, M. Ohlsson, E. Holmgren, S. Josephsson, and S. S. Alkan. Three human interferon-alpha 2 subvariants disclose structural and functional differences. *Eur. J. Biochem.* **190**:257–261 (1990).
20. E. N. Fish, K. Banerjee, and N. Stebbing. Human leukocyte interferon subtypes have different anti-proliferative and anti-viral activities on human cells. *Biochem. Biophys. Res. Commun.* **112**:537–546 (1983).
21. K. Oberg and G. Alm. The incidence and clinical significance of antibodies to interferon-a in patients with solid tumors. *Biotherapy* **10**:1–5 (1997).
22. R. Siemers, L. Hensley, and H. Ozer. Localization of the receptor binding site of IFN-α2b. *J. Immunol.* **141**:1550–1555 (1988).
23. U. K. Laemmli. Cleavage of structural proteins during the assembly of the head of bacteriophage T4. *Nature* **227**:680–685 (1970).

24. M. M. Kurfurst. Detection and molecular weight determination of polyethylene glycol-modified hirudin by staining after sodium dodecyl sulfate-polyacrylamide gel electrophoresis. *Anal. Biochem.* **200**:244–248 (1992).

25. G. E. Sims and T. J. Snape. A method for the estimation of polyethylene glycol in plasma protein fractions. *Anal. Biochem.* **107**:60–63 (1980).

26. S. Cruz, C. Duarte, E. Ferra, G. Fontirroche, J. Vázquez, L. Martínez, N. Arteaga, E. Perez, and J. Gavilondo. Quantification of human recombinant IFN-α2b by monoclonal antibodies. *Biotecnol. Apl.* **7**:132–141 (1990).

27. H. Santana, Y. Espino, A. Franco, G. Furrazola, and E. Hardy. A sandwich-type enzyme-linked immunosorbent assay for the analysis of recombinant human interferon α-2b. *Biotechnol. Tech.* **13**:341–346 (1999).

28. J. Ferrero, M. E. Ochagavia, A. Aguilera, and P. López-Saura. Interferon antiviral activity titration using the "SUMA" device system. *Biotecnol. Apl.* **11**:34–42 (1994).

29. H. Akaike. Canonical correlation analysis of time series and the use of an information criterion. In R. K. Mehra and D. G. Lairriotis (eds.), *System Identification: Advances and Case Studies*, Academic Press, New York, 1976, pp. 52–107.

30. D. Perrier and M. Gibaldi. Related general derivation of the equation for time to reach a certain fraction of steady state. *J. Pharm. Sci.* **71**:474–475 (1982).

31. GraphPad Prism 4 user's guide. http://www.graphpad.com/manuals/Prism4/PrismUsersGuide.pdf (accessed 01/02/05).

32. S. Zalipsky and C. Lee. Use of functionalized poly(ethylene glycol)s for modification of polypeptides. In J. M. Harris (ed.), *Poly(Ethylene Glycol) Chemistry: Biotechnical and Biomedical Applications*, Plenum Press, New York, 1996, pp. 347–381.

33. P. Bailon and A. Palleroni. European Patent No. 0 809 996 (1997).

34. M. Diwan and T. G. Park. Stabilization of recombinant interferon-alpha by pegylation for encapsulation in PLGA microspheres. *Int. J. Pharm.* **252**:111–122 (2003).

35. M. Morpurgo and F. M. Veronese. Conjugates of peptides and proteins to polyethylene glycols. *Methods Mol. Biol.* **283**:45–70 (2004).

36. B. D. Hames and D. Rickwood. *Gel Electrophoresis of Proteins. A Practical Approach*, IRL Press, New York, 1990.

37. J. E. Seely and C. W. Richey. Use of ion-exchange chromatography and hydrophobic interaction chromatography in the preparation and recovery of polyethylene glycol-linked proteins. *J. Chromatogr. A* **908**:235–241 (2001).

38. S. P. Monkarsh, Y. Ma, A. Aglione, P. Bailon, D. Ciolek, B. DeBarbieri, M. C. Graves, K. Hollfelder, H. Michel, A. Palleroni, J. E. Porter, E. Russoman, S. Roy, and Y. C. Pan. Positional isomers of monopegylated interferon alpha-2a: isolation, characterization, and biological activity. *Anal. Biochem.* **247**:434–440 (1997).

39. S. Foser, A. Schacher, K. A. Weyer, D. Brugger, E. Dietel, S. Marti, and T. Schreitmuller. Isolation, structural characterization, and antiviral activity of positional isomers of monopegylated interferon alpha-2a (PEGASYS). *Protein Expr. Purif.* **30**:78–87 (2003).

40. P. K. Smith, R. I. Krohn, G. T. Hermanson, A. K. Mallia, F. H. Gartner, M. D. Provenzano, E. K. Fujimoto, N. M. Goeke, B. J. Olson, and D. C. Klenk. Measurement of protein using bicinchoninic acid. *Anal. Biochem.* **150**:76–85 (1985).

41. K. J. Wiechelman, R. D. Braun, and J. D. Fitzpatrick. Investigation of the bicinchoninic acid protein assay: identification of the groups responsible for color formation. *Anal. Biochem.* **175**:231–237 (1988).

42. J. M. Harris and R. B. Chess. Effect of pegylation on pharmaceuticals. *Nat. Rev. Drug Discov.* **2**:214–221 (2003).

43. P. Bailon and W. Berthold. Poly(ethylene glycol)-conjugated pharmaceutical proteins. *Pharm. Sci. Technol. Today* **1**:352–356 (1998).

44. K. D. Hinds and S. W. Kim. Effects of PEG conjugation on insulin properties. *Adv. Drug Deliv. Rev.* **54**:505–530 (2002).

45. O. B. Kinstler, D. N. Brems, S. L. Lauren, A. G. Paige, J. B. Hamburger, and M. J. Treuheit. Characterization and stability of N-terminally PEGylated rhG-CSF. *Pharm. Res.* **13**:996–1002 (1996).

46. W. Li, Y. Wang, X. Zhu, M. Li, and Z. Su. Preparation and characterization of PEGylated adducts of recombinant human tumor necrosis factor-alpha from *Escherichia coli. J. Biotechnol.* **92**:251–258 (2002).

47. H. Lee, I. H. Jang, S. H. Ryu, and T. G. Park. N-terminal site-specific mono-PEGylation of epidermal growth factor. *Pharm. Res.* **20**:818–825 (2003).